

RECEIVED BY OST

APR 21 1985

CONF-8412

M85010251

CONF-841210--23

DE85 010251

**TRU DECONTAMINATION OF HIGH-LEVEL PUREX WASTE BY SOLVENT EXTRACTION USING A MIXED OCTYL(PHENYL)-N,N-DIISOBUTYL-CARBAMOYLMETHYLPHOSPHINE OXIDE/TBP/NPH (TRUEX) SOLVENT**

**E. Philip Horwitz, Dale G. Kalina, Herbert Diamond, and Louis Kaplan**

**Chemistry Division, Argonne National Laboratory, Argonne, IL 60439**

**George F. Vandegrift,\* Ralph A. Leonard, and Martin J. Steindler**

**Chemical Technology Division, Argonne National Laboratory, Argonne, IL 60439**

**Wallace W. Schulz**

**Rockwell Hanford Operations, Richland, WA 99352**

**ABSTRACT**

The TRUEX (transuranium extraction) process was tested on a simulated high-level dissolved sludge waste (DSW). A batch counter-current extraction mode was used for seven extraction and three scrub stages. One additional extraction stage and two scrub stages and all strip stages were performed by batch extraction. The TRUEX solvent consisted of 0.20 M octyl(phenyl)-N,N-diisobutylcarbamoymethylphosphine oxide-1.4 M TBP in Conoco (C<sub>12</sub>-C<sub>14</sub>). The feed solution was 1.0 M in HNO<sub>3</sub>, 0.3 M in H<sub>2</sub>C<sub>2</sub>O<sub>4</sub> and contained mixed (stable) fission products, U, Np, Pu, and Am, and a number of inert constituents, e.g., Fe and Al. The test showed that the process is capable of reducing the TRU concentration in the DSW by a factor of 4 x 10<sup>4</sup> (to <100 nCi/g of disposed form) and reducing the quantity of TRU waste by two orders of magnitude.

**MASTER**

**DISCLAIMER**

This report was prepared as an account of work sponsored by an agency of the United States Government. Neither the United States Government nor any agency thereof, nor any of their employees, makes any warranty, express or implied, or assumes any legal liability or responsibility for the accuracy, completeness, or usefulness of any information, apparatus, product, or process disclosed, or represents that its use would not infringe privately owned rights. Reference herein to any specific commercial product, process, or service by trade name, trademark, manufacturer, or otherwise does not necessarily constitute or imply its endorsement, recommendation, or favoring by the United States Government or any agency thereof. The views and opinions of authors expressed herein do not necessarily state or reflect those of the United States Government or any agency thereof.

\* Author to whom reprint request should be sent.

## 1. INTRODUCTION

Nitric acid solutions of high-level waste (HLW) are produced during the processing of irradiated nuclear fuel by the PUREX process. In some cases, the HLW is made alkaline and stored in large underground tanks. Neutralized HLW contains both a liquid and solid (sludge) phase. Sludge is primarily a mixture of hydroxides or hydrated oxides of nonradioactive elements (e.g.,  $\text{Fe}_2\text{O}_3 \cdot x\text{H}_2\text{O}$ ), but also contains essentially all the  $^{90}\text{Sr}$ , fission product lanthanides, uranium, and transuranic (TRU) elements (Np, Pu, Am) present in the HLW. Dissolution of the sludge in an oxalic-nitric acid mixture creates HLW that we refer to as dissolved sludge waste (DSW).

This paper reports the results of batch countercurrent tests of a solvent extraction flowsheet designed to remove and concentrate the TRU from DSW. If the TRU content of the DSW stream can be lowered to  $<100$  nCi/g of solid, it can be classified as nonTRU.<sup>1]</sup> If, in addition,  $^{90}\text{Sr}$  levels in the DSW can be reduced, it will be eligible for near-surface disposal. In the case of DSW, this would mean that only the TRU concentrate product of a separation process ( $\leq 1$  wt % of the initial mass) would need to be buried in a deep geologic disposal site.

The TRUEX solvent extraction process, which has been reported elsewhere<sup>2,3]</sup>, is based on the use of a neutral, bifunctional, phosphorus-based extractant dissolved in tributyl phosphate (TBP) diluted by a normal paraffinic hydrocarbon (NPH). Octyl(phenyl)-N,N-diisobutylcarbamoylmethylphosphine oxide ( $\text{O}\phi\text{D}[\text{IB}]\text{CMPO}$ ), illustrated in Figure 1, is the bifunctional extractant that was determined to be the best candidate for the TRUEX process based on (1) its relatively high values of the distribution ratio of americium ( $D_{\text{Am}}$ ) over 0.5 to 5 M nitric acid concentration, (2) its good selectivity for Am(III) over fission products and inert elements, (3) its ability to reach high loadings without third

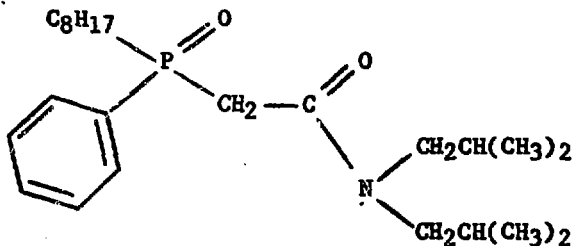


Figure 1. Extractant O D[1B]CMPO

phase formation when mixed with PUREX process solvent, and (4) its ease of synthesis and availability in high purity. A comprehensive report on the use of the TRUEX process for TRU removal from HLW and DSW is given.<sup>2]</sup> The generic TRUEX solvent extraction process and its underlying chemistry are described.<sup>3]</sup> A batch countercurrent experiment was conducted to (1) test the ability of the TRUEX process to decontaminate a synthetic DSW solution from americium, plutonium, and neptunium when operated in a countercurrent mode; (2) look for interfacial crud buildup or phase disengagement problems; and (3) determine the behavior of a number of fission-product and inert elements in extraction and scrub stages.

## 2. EXPERIMENTAL PROCESS

### 2.1 Materials

The composition of synthetic DSW solution is described in Tables I, II, and III. Its preparation is described in detail.<sup>2]</sup> Analyses were conducted using inductively coupled plasma/atomic emission spectrometry (ICP/AES). A nonradioactive DSW solution was prepared initially for cold testing. Americium (<sup>241</sup>Am), plutonium (<sup>242</sup>Pu), neptunium (<sup>237</sup>Np and <sup>239</sup>Np), and technetium (<sup>99</sup>Tc) were added to a portion of the DSW for hot testing of the flowsheet. In addition, a second radionuclide-containing solution

**TABLE I****COMPOSITION OF THE SYNTHETIC DSW:  
NONFISSION PRODUCTS**

Constituent	Concentration, M	
	Added	Found <sup>a,b</sup>
HNO <sub>3</sub>	1.0	NA
Na	0.15	NA
Mg	0.0016	0.0017
Al	0.046	0.045
Ca	0.0014	0.0014
Cr	0.014	0.013
Mn	0.0045	0.0047
Fe	0.15	0.15
Ni	0.0080	0.0086
Cu	0.0018	0.0019
F <sup>-</sup>	0.008	NA
SO <sub>4</sub> <sup>2-</sup>	0.012	NA
H <sub>2</sub> C <sub>2</sub> O <sub>4</sub>	0.30	NA
NO <sub>2</sub> <sup>-c</sup>	0.005	NA

<sup>a</sup>NA means not analyzed.

<sup>b</sup>These ICP/AES analyses have a 3-10% error range; the magnitude of the error is a function of the element's concentration and the degree of interference from other elements.

<sup>c</sup>On addition of solid NaNO<sub>2</sub> to the feed, some reddish-brown gas (likely NO<sub>x</sub>) was released.

was prepared with a higher <sup>237</sup>Np concentration for use in a three-stage countercurrent experiment that measured the effect of the feed concentration of neptunium on its solvent extraction behavior.

TABLE II

COMPOSITION OF SYNTHETIC DSW SOLUTION:  
FISSION PRODUCTS

Constituent	Concentration, M	
	Added	Found <sup>a, b</sup>
Se	$9.5 \times 10^{-5}$	$<1.6 \times 10^{-4c}$
Sr	$1.4 \times 10^{-3}$	$1.4 \times 10^{-3}$
Y	$7.3 \times 10^{-4}$	$7.0 \times 10^{-4}$
Zr	$5.6 \times 10^{-3}$	$6.2 \times 10^{-3}$
Mo	$1.8 \times 10^{-4}$	$1.6 \times 10^{-4}$
Tc	$1.0 \times 10^{-5}$	$9.6 \times 10^{-6d}$
Ru	$2.1 \times 10^{-3}$	$2.0 \times 10^{-3}$
Rh	$5.7 \times 10^{-4}$	$5.7 \times 10^{-4}$
Pd	$5.4 \times 10^{-4}$	$6.6 \times 10^{-4}$
Ag	$3.6 \times 10^{-5}$	$3.0 \times 10^{-5}$
Cd	$5.0 \times 10^{-5}$	$4.4 \times 10^{-5}$
Te	$3.3 \times 10^{-4}$	$3.3 \times 10^{-4}$
Ba	$1.1 \times 10^{-3}$	$2.1 \times 10^{-4e}$
La	$1.0 \times 10^{-3}$	$9.5 \times 10^{-4}$
Ce	$2.4 \times 10^{-3}$	$2.3 \times 10^{-3}$
Pr	$9.2 \times 10^{-4}$	$8.6 \times 10^{-4}$
Nd	$2.7 \times 10^{-3}$	$2.6 \times 10^{-3}$
Sm	$3.9 \times 10^{-4}$	$3.8 \times 10^{-4}$
Eu	$4.8 \times 10^{-5}$	$4.9 \times 10^{-5}$
Gd	$1.2 \times 10^{-5}$	NA

<sup>a</sup>NA means not analyzed.

<sup>b</sup>These ICP/AES analyses have a 3-10% error range; the magnitude of the error is a function of the element's concentration and the degree of interference from other elements.

<sup>c</sup>The amount added to solution was below its ICP/AES detectability.

<sup>d</sup>Based on radiochemical analysis of  $^{99}\text{Tc}$ .

<sup>e</sup>The low concentration of Ba ion is due to its precipitation as  $\text{BaSO}_4$ .

TABLE III

COMPOSITION OF SYNTHETIC DSW FEED SOLUTIONS:  
ACTINIDES

Constituent	Concentration, <u>M</u>	Activity, dpm/L
238U	$1 \times 10^{-4}$	$2 \times 10^4$
$^{237}\text{Np}$ - $^{239}\text{Np}$ <sup>a</sup>	$1.0 \times 10^{-6}$ <sup>b</sup>	$9 \times 10^8$ <sup>c</sup>
242Pu	$1.6 \times 10^{-6}$	$3.3 \times 10^6$
241Am	$7.0 \times 10^{-6}$	$1.3 \times 10^{10}$

<sup>a</sup>The bulk of the Np concentration was as  $^{237}\text{Np}$ ; the bulk of its radioactivity was due to  $^{239}\text{Np}$ .

<sup>b</sup>For a separate three-stage countercurrent experiment the concentration of  $^{237}\text{Np}$  was increased to  $2 \times 10^{-4}$ .

<sup>c</sup>Activity level at the start of the experiment; the activities of all samples were corrected to this time based on the short half-life of  $^{239}\text{Np}$  (2.35 days).

The preparation of the TRUEX process solvent (0.2 M O $\phi$ D[1B]CMPO-1.4 M TBP-NPH\*) is described in detail,<sup>2]</sup> as are the preparations of all other scrub and strip solutions used in this experiment. The compositions of these solutions are:

Scrub 1	2.5 <u>M</u> HNO <sub>3</sub> - 0.06 <u>M</u> H <sub>2</sub> C <sub>2</sub> O <sub>4</sub> *
Scrub 2	0.5 <u>M</u> HNO <sub>3</sub> - 0.01 <u>M</u> Fe(NO <sub>3</sub> ) <sub>3</sub>
Strip 1	0.01 <u>M</u> HNO <sub>3</sub> - 0.005 <u>M</u> HAN <sup>†</sup>
Strip 2	0.1 <u>M</u> H <sub>2</sub> C <sub>2</sub> O <sub>4</sub>

The bases for selecting these solutions are discussed.<sup>2,3]</sup>

\*The NPH used was Conoco C<sub>12</sub>-C<sub>14</sub>, with an average carbon chain length of 13.2.

\*\*H<sub>2</sub>C<sub>2</sub>O<sub>4</sub> = oxalic acid.

<sup>†</sup>HAN = hydroxylammonium nitrate.

## 2.2 The Countercurrent Experiments

The experiments were performed in a series of ten 100-ml, water-jacketed, separatory funnels with flared tops (to permit easy pouring of liquids into them). The phases in each funnel were mixed by a stainless steel centrifugal agitator rotated by a light-duty, variable-speed motor. The funnels were thermostated to  $40 \pm 1^\circ\text{C}$ .

Figure 2 shows the flow design of the countercurrent experiments, which were performed in the "double-diamond" mode described by Peppard.<sup>4</sup> This was done to ensure simplicity of operation and adequate volumes of raffinate and loaded-organic samples for later experiments.

For the cold run, the feed, organic, and scrub solutions were added to the experiment at the appropriate stages shown in Figure 2. When solutions had been transferred to each funnel, they were allowed to come to thermal equilibrium for about two minutes and were then stirred for about one minute. The stirring speed was set by visually observing complete dispersion of phases in each funnel. After stirring was complete and the phases completely disengaged, the aqueous and organic phases were removed from each funnel and set aside until this part of the operation was complete. Following the diagram of Figure 2, each organic phase was transferred one separatory funnel to the right and each aqueous phase one funnel to the left. Fresh feed, scrub 1, scrub 2, and organic solvent were added at their proper stages and the procedure was repeated, all ten stages running simultaneously.

Samples of loaded organic phase and aqueous phase from stages 10 and 1, respectively, were collected during the course of the experiment. At the end of the cold run, portions of the organic phase and aqueous phase were removed from every stage. The remaining organic and aqueous phases were allowed to sit in the separatory funnels overnight.

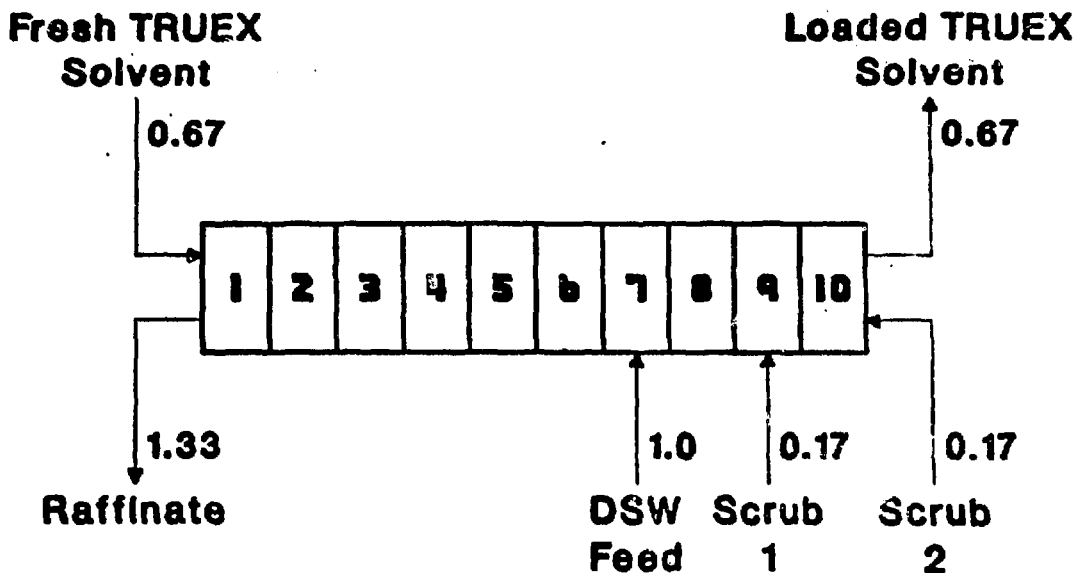


Figure 2. The experimental design and flow ratios of the counter-current experiment. (Boxes numbered 1-10 represent the separatory funnels or stages; numbers alongside arrows indicate relative flow rates.)

The hot run was conducted by substituting the radioisotope-containing feed for the cold feed used the previous day. The volumes of the feed, organic, and two scrub solutions were all reduced proportionally to match the lower volumes of the solutions in the ten stages.

After the requisite number of feeds had passed through the system to reach the calculated >90%-of-steady-state condition for [ $^{241}\text{Am}$ ] in the raffinate, the separatory funnels were drained and the organic and aqueous phases were separated and labeled for further testing and analysis.



## 2.3 Batch Experiments

The additional steps listed here followed the countercurrent experiments:

2.3.1 Stage 0. A sample was removed from the aqueous phase of stage 1, and the remainder was contacted with fresh organic phase.

2.3.2 Scrub stages 11, 12, and 13. The last two loaded organic phases from the hot run that left the system prior to shutdown were combined and equilibrated with three additional portions of fresh scrub 2 in an organic/aqueous (O/A) phase ratio of 4:1.

2.3.3 Stripping. The loaded organic phase from stage 13 was mixed with strip solution 1 for one minute in an O/A phase ratio of 2:1 for six and ten consecutive strips for the cold and hot runs, respectively. For the cold run, a sample of each strip solution was tested for the presence of lanthanides by the addition of oxalic acid, whereas the progress of americium and neptunium stripping was monitored by removing small aliquots of the organic phase for gamma analysis between strips. After an average of seven strips, the resultant organic phase was divided. Part was saved and part was stripped further by strip solution 2. The strip solutions from the first seven consecutive contacts of the organic phase were combined for further technetium and plutonium analyses.

## 2.4 A Second Hot Countercurrent Experiment

An ancillary experiment was performed after the analysis of data showed that the decontamination factor for neptunium in the countercurrent experiment was a disappointing value of 6, and the efficiency of stripping neptunium was low. It was hypothesized

that the low neptunium extraction was due to the relatively low concentration of neptunium in the feed (Table III). To test this hypothesis, a three-stage countercurrent experiment was undertaken with the same equipment and volumes as the first hot countercurrent experiment. The feed stage was again stage 7; both scrub solutions were combined in stage 8; and the TRUEX solvent entered at stage 6. Because of the limited volume of feed, a single-diamond experiment was run in which the addition of feed in stage 7 was alternated with the addition of solvent and scrub in stages 6 and 8. Four raffinate samples were collected before shutdown, after which the organic and aqueous phases from each stage were collected for analysis.

## 2.5 Distribution-Ratio Measurements

The distribution ratios of the nonradioactive constituents of DSW were measured by analyzing samples of the organic and aqueous phases from each stage at the conclusion of the cold countercurrent test run. Multielement analysis was performed using ICP/AES, as described in previous publications.<sup>2,3,5</sup> The distribution ratios  $D_{\text{H}_2\text{C}_2\text{O}_4}$  and  $D_{\text{Tc}}$  were measured by spiking samples of aqueous phase from the cold run with  $^{14}\text{C}$ -labeled oxalic acid and  $^{99}\text{Tc}$  and equilibrating them with samples of the corresponding organic phase at  $40^\circ\text{C}$  for four minutes. The  $^{14}\text{C}$  and  $^{99}\text{Tc}$  concentrations were measured using standard scintillation counting techniques, and  $D_{\text{Am}}$  and  $D_{\text{Np}}$  were measured using standard gamma counting techniques. Analyses of uranium and plutonium in the aqueous phase were performed by laser excitation fluorescence spectroscopy and isotopic dilution analysis, respectively. The values of  $D_{\text{U}}$  and  $D_{\text{Pu}}$  were then calculated based on mass balance between stages.

## 2.6 Methods of Flowsheet Design

Calculations for flowsheet design were made by either standard equations or use of the McCabe-Thiele method. The graphical technique of the McCabe-Thiele method was especially useful when distribution ratios of DSW components varied from stage to stage and when insight was needed into the effect of more stages on the improvement of separations. Specifics of flowsheet design may be found.<sup>2,6]</sup>

Because the batch countercurrent experiment was labor intensive and the amount of feed material was limited, it was important to know how quickly the aqueous raffinate concentration of americium reached a value sufficient to make the DSW raffinate a nonTRU waste. Because the McCabe-Thiele method works only for steady-state operation, it could not be used here. A method to determine the approach of the raffinate to a steady-state concentration is the use of step-by-step calculations.<sup>7,8]</sup> These calculations are normally tedious; however, we found that the computation is greatly simplified by use of electronic spreadsheets. Using the DIGICALC electronic spreadsheet (WHY Systems, Inc., Redmond, WA), the rate at which the americium concentration in the aqueous raffinate approached its steady-state value was calculated. These calculations, which give the concentration for each step\* and each stage of the run can be continued until steady-state concentrations are reached at each stage. Besides giving steady-state concentrations, this alternative calculational method incorporates other features of the McCabe-Thiele method; e.g., different distribution coefficients can be used for each stage and two scrub sections can be evaluated for an extraction/scrub unit.

---

\*That is, each liquid-liquid equilibration in a stage; thus, a "step" corresponds to one residence time in a stage.

### 3. RESULTS

The conceptual flowsheet for TRU removal and concentration from DSW was designed to reduce the activity level of TRU elements in the aqueous raffinate of the TRUEX process to  $\leq 100$  nCi/g solidified raffinate. Based on the initial composition of the DSW feed and the projected partitioning of its components, 1 L of feed would produce 230 g of solidified raffinate. Table IV presents the composition of solidified raffinate and mass of major constituents. The predicted activity levels of TRU elements in DSW and the decontamination factors achieved in the batch countercurrent experiment are presented in Table V, which also shows the specific alpha activity contained in the solidified raffinate and in a grout containing 20 wt % solidified raffinate. Table VI presents the composition of the TRU product. Clearly, this experiment has proven the effectiveness of the TRUEX solvent extraction process to reduce the TRU content of the raffinate below prescribed limits. Specific details of the experiment follows.

#### 3.1 Actinide Behavior

Figures 3, 4, and 5 show the aqueous- and organic-phase concentrations of americium, neptunium, and plutonium in each stage of the countercurrent experiment at their near-steady-state conditions. Figure 3 also shows americium data for the final batch extraction stage (stage 0). Data for batch scrubbing stages 11-13 are shown for americium and neptunium in Figures 3 and 4. The plutonium concentration was below its detectability limit in the aqueous phases in stages 1-3.

Table VII presents distribution ratios for the TRU elements and uranium. The solvent extraction behaviors of both americium and plutonium were consistent with those expected from earlier batch experiments. Both elements demonstrated well-behaved extraction characteristics from stage to stage and attained

TABLE IV

SOLIDIFIED RAFFINATE COMPOSITION AND MASS  
OF CONSTITUENTS PER VOLUME OF FEED

Component	Mass of Component per Liter of Feed, g
$\text{NaNO}_3^a$	138.52
$\text{Na}_2\text{SO}_4$	1.51
$\text{Fe}(\text{NO}_3)_3 \cdot 9\text{H}_2\text{O}$	60.75
$\text{FePO}_4 \cdot 4\text{H}_2\text{O}$	0.72
$\text{Mg}(\text{NO}_3)_2 \cdot 6\text{H}_2\text{O}$	0.26
$\text{Al}(\text{NO}_3)_3 \cdot 9\text{H}_2\text{O}$	16.26
$\text{Al}_2\text{F}_6 \cdot 7\text{H}_2\text{O}$	0.39
$\text{CaSO}_4$	0.18
$\text{Cr}(\text{NO}_3)_3 \cdot 9\text{H}_2\text{O}$	5.04
$\text{Mn}(\text{NO}_3)_2 \cdot 6\text{H}_2\text{O}$	1.29
$\text{Ni}(\text{NO}_3)_2 \cdot 6\text{H}_2\text{O}$	2.33
$\text{Cu}(\text{NO}_3)_2 \cdot 6\text{H}_2\text{O}$	0.52
$\text{Zr}(\text{NO}_3)_4 \cdot 5\text{H}_2\text{O}$	2.40
$\text{Ba}(\text{NO}_3)_2$	<u>0.29</u>
Total	230.46

<sup>a</sup>Includes the  $\text{NaNO}_3$  formed when the 1.5 mol of  $\text{HNO}_3$  in 1.33 L of raffinate are neutralized with  $\text{NaOH}$ .

distribution ratios that were high enough to easily achieve requisite concentration levels in the raffinate. The small effect of loading on  $D_{Am}$  in the extraction section makes predictions of extraction parameters both simple and trustworthy. The  $D_{Pu}$  value reflects the complexing of plutonium in the aqueous phase by oxalic acid;  $D_{Pu}$  was measured to be much higher from nitric acid solution alone than it was from DSW feed.

TABLE V

## SUMMARY OF CALCULATIONS FOR TRU CONTENT OF SOLIDIFIED RAFFINATE

Radio-nuclide	Activity in Feed, nCi/L	Decontamination Factor <sup>a</sup>	Activity in Solidified Raffinate, <sup>b</sup> nCi/g	Activity in Grout, <sup>c</sup> nCi/g
Am	1 x 10 <sup>8</sup>	1.0 x 10 <sup>4</sup> <sup>c</sup>	40	8
Pu	2 x 10 <sup>4</sup>	>1 x 10 <sup>5</sup>	<2 x 10 <sup>-3</sup>	-
Np	4 x 10 <sup>4</sup>	6	30	6
Total	1 x 10 <sup>8</sup>	-	70	14

<sup>a</sup>This is the measured decontamination factor for the raffinate from stage 1 of the countercurrent experiment. This was followed by a batch contact of the raffinate with fresh TRUOX solvent (stage 0) that increased the factor for americium to 4.6 x 10<sup>4</sup>.

<sup>b</sup>If the stage 0 decontamination factor were used, the americium specific activity would drop to 9 nCi/g and the total specific activity to 40 nCi/g.

<sup>c</sup>If the stage 0 decontamination factor were used, the americium specific activity would drop to 2 nCi/g and the total specific activity to 8 nCi/g.

TABLE VI

## COMPOSITION OF TRU PRODUCT

Element	Form of Oxide	Mass of Oxide per Liter of Feed, g
La	La <sub>2</sub> O <sub>3</sub>	0.15
Ce	CeO <sub>2</sub>	0.39
Pr	Pr <sub>6</sub> O <sub>11</sub>	0.14
Nd	Nd <sub>2</sub> O <sub>3</sub>	0.45
Sm	Sm <sub>2</sub> O <sub>3</sub>	0.07
Eu	Eu <sub>2</sub> O <sub>3</sub>	0.01
Y	Y <sub>2</sub> O <sub>3</sub>	0.08
Fe	Fe <sub>2</sub> O <sub>3</sub>	0.03
Ru	RuO <sub>2</sub>	0.02
Rh	Rh <sub>2</sub> O <sub>3</sub>	0.01
Pd	PdO	0.01
Np, Pu, Am	(Np, Pu, Am) <sub>2</sub> O <sub>3</sub>	0.12
		1.5

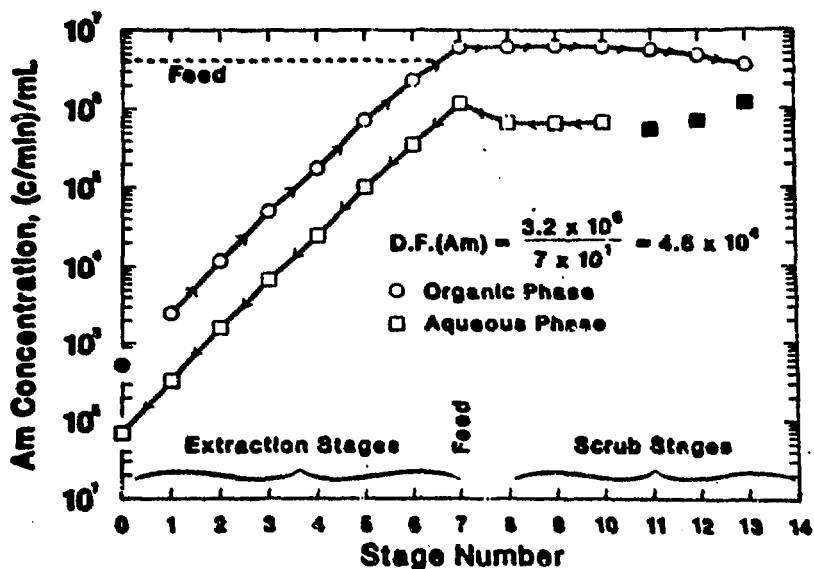


Figure 3. Americium concentration in the organic and aqueous phases in each stage of the countercurrent experiment at near-steady-state condition. (Darkened symbols, not connected by line, are batch contacts.)

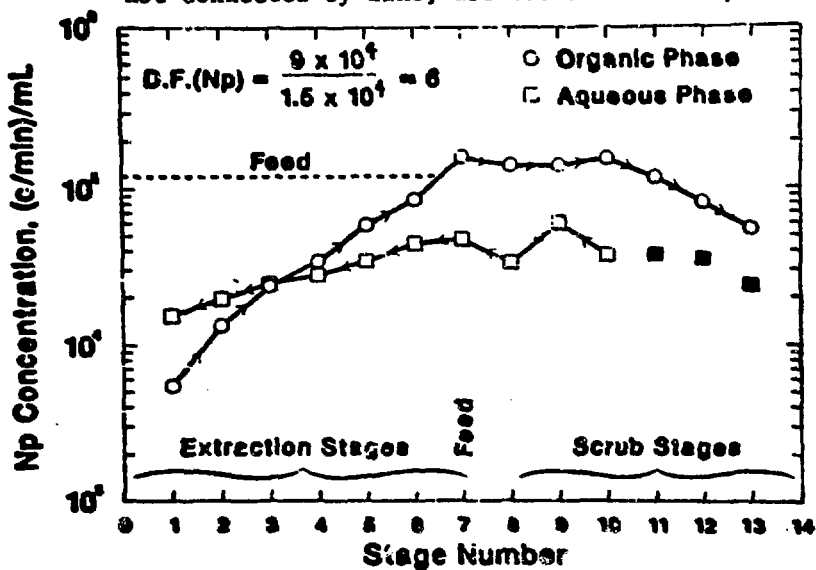


Figure 4. Neptunium concentration in the organic and aqueous phases in each stage of the countercurrent experiment at near-steady-state condition. (Darkened symbols, not connected by line, are batch contacts.)

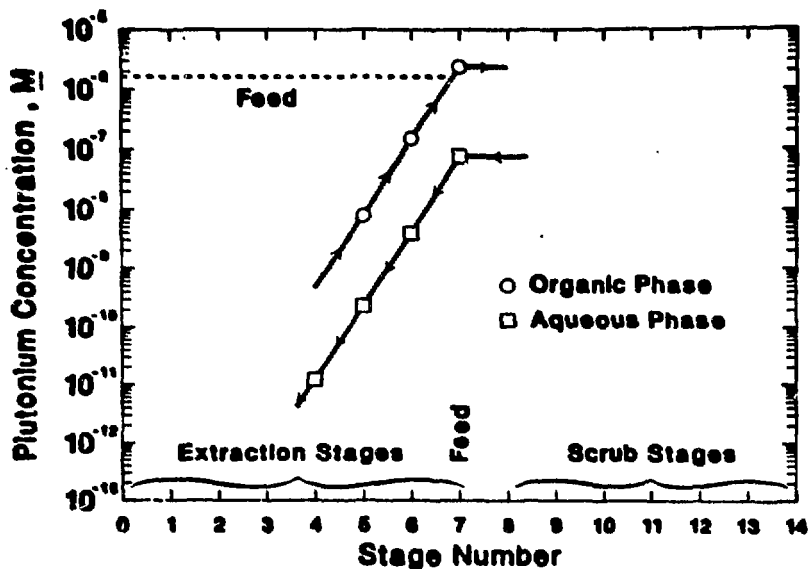


Figure 5. Plutonium concentration in the organic and aqueous phases in each stage of the countercurrent experiment at near-steady-state condition.

The behavior of neptunium (Figure 4 and Table VII) was disappointing. Although neptunium was added to the synthetic DSW as Np(V), and  $\text{NaNO}_2$  was added to further stabilize the Np(V), the high concentration of oxalic acid was expected to shift the disproportionation of Np(V) to Np(IV) and Np(VI) because, like Pu(IV), Np(IV) is strongly complexed by oxalic acid. Inasmuch as Np(VI) is reduced rapidly to Np(V) by oxalic acid, Np(V) should transform to Np(IV) in DSW. Because the majority (86%) of the neptunium was extracted, the disproportionation did proceed as described above (but not to the extent that was expected). The consistency of  $D_{\text{Pu}}$  from stage to stage indicates that only one oxidation state of plutonium is present in the aqueous phase. On the other hand, the decrease in  $D_{\text{Np}}$  from stage to stage suggests the presence of Np(V) and Np(IV) species.

The three-stage (two extraction and one scrub) countercurrent experiment was performed to determine whether increasing the concentration of neptunium by two orders of magnitude would



TABLE VII

DISTRIBUTION RATIOS OF ACTINIDE ELEMENTS IN EACH STAGE  
OF THE COUNTERCURRENT EXPERIMENT

Stage <sup>b</sup>	Distribution Ratio <sup>a</sup>			
	U <sup>c</sup>	Np	Pu <sup>c</sup>	Am
0	NA	NA	NA	7.6
1	NA	0.36	NA	7.5
2	NA	0.68	NA	7.4
3	NA	0.96	NA	7.3
4	NA	1.2	NA	7.2
5	NA	1.7	34	7.1
6	<10 <sup>2</sup>	1.9	39	6.5
7	2.6 x 10 <sup>2</sup>	3.3	32	5.2
8	5.1 x 10 <sup>2</sup>	4.2	NA	9.4
9	6.1 x 10 <sup>2</sup>	2.3	NA	9.7
10	6.5 x 10 <sup>2</sup>	4.1	NA	9.1
11	6.5 x 10 <sup>2</sup>	3.1	NA	10.0
12	NA	2.3	NA	6.7
13	NA	2.3	NA	3.0

<sup>a</sup>NA means not analyzed.

<sup>b</sup>Stage 7 is the feed stage; stages 0-7 are extraction stages; stages 8 and 9 are scrub 1 stages; and stages 10-13 are scrub 2 stages.

<sup>c</sup>Organic-phase concentrations were not measured; distribution ratios were estimated by material balance.

increase the transformation of Np(V) to Np(IV). The rationale for this hypothesis was that the rate of disproportionation of Np(V) would increase at the higher concentration. The relative volumes of feed, scrub, and organic solutions were the same as in the ten-stage experiment. The effect of higher concentration appeared to be minimal; complete data are presented elsewhere.<sup>2]</sup>

Figures 6 and 7 show the approach of americium and neptunium to steady state in the batch countercurrent experiment. The line in each figure was calculated using the experimental distribution ratios presented in Table VII and the spreadsheet calculation. These calculations assumed a 3% increase in the volume of the

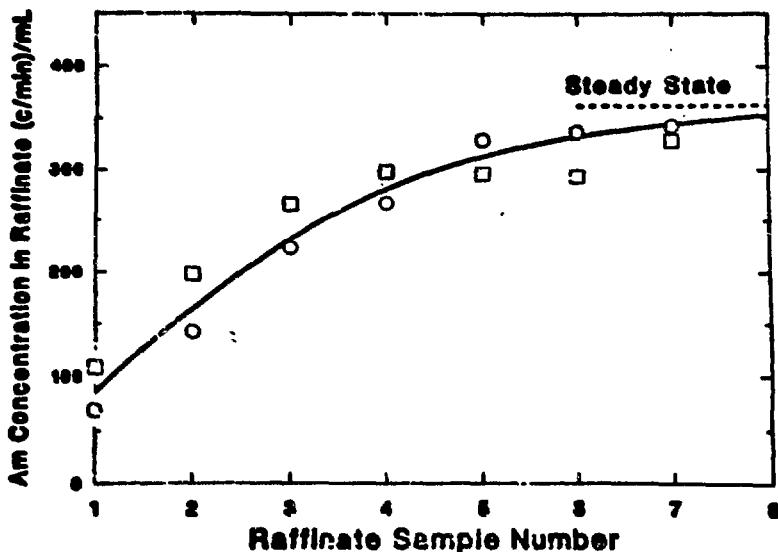


Figure 6. Americium concentration in a raffinate sample vs. the raffinate sample number. The data points are raffinate samples of the double-diamond countercurrent experiment (the two sets of samples are differentiated by symbol type); the line is calculated based on the near-steady-state distribution ratios measured for each stage of the experiment.

organic phase (as a result of loading) relative to that of the aqueous phase. The good fit between the curve derived from distribution-ratio measurements and the raffinate data indicates a consistency in the experiment that makes an extrapolation to steady-state conditions valid. The steady-state decontamination factors for the TRU elements in this experiment are presented in Table VIII.

### 3.2 Nonactinide Behavior

The distribution ratios for the nonactinide constituents in the extraction and scrub stages at near-steady-state conditions are presented in Tables IX and X. The near-steady-state values

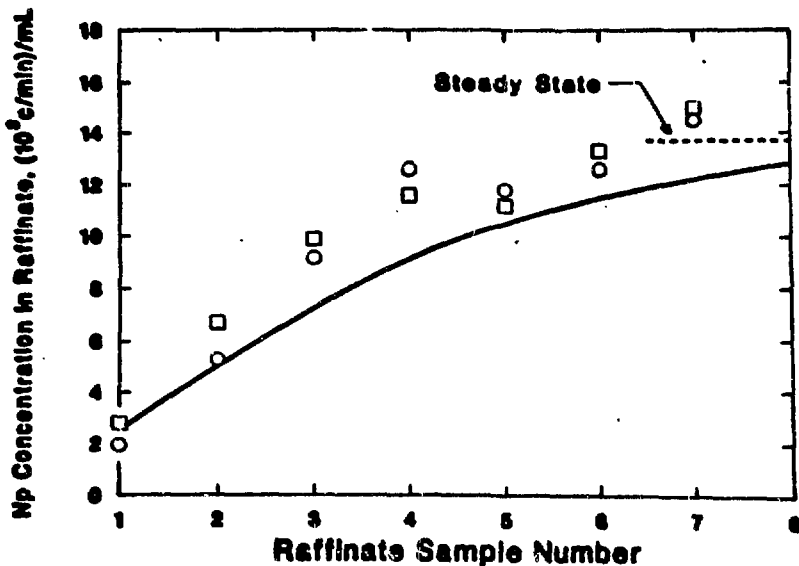


Figure 7. Neptunium concentration in a raffinate sample vs. the raffinate sample number. The data points are raffinate samples of the double-diamond countercurrent experiment (the two sets of samples are differentiated by symbol type); the line is calculated based on the near-steady-state distribution ratios measured for each stage of the experiment.

TABLE VIII

STEADY-STATE DECONTAMINATION FACTORS OF TRU ELEMENTS AND URANIUM FROM SIMULATED DSW

Element	Number of Extraction Stages to Attain Measured Factor	Measured Factor	Factor Calculated for Measured After Seven Extraction Stages
U	2	$1.3 \times 10^4$	$1.0 \times 10^{16}{}^a$
Np	7	6	6
Pu	4	$1.0 \times 10^5$	$5.0 \times 10^{14}{}^a$
Am	8	$4.6 \times 10^4$	$1.0 \times 10^4$

<sup>a</sup>Because stripping of solvent is never perfect, some residual concentration of these species will be in the recycled solvent; therefore, these values would not be achieved in actual practice.

TABLE IX

**DISTRIBUTION RATIOS OF NONFISSION PRODUCTS IN EACH STAGE OF THE COUNTERCURRENT EXPERIMENT**

Stage No. <sup>c</sup>	Distribution Ratio a,b								
	H <sub>2</sub> O <sub>x</sub> <sup>d</sup>	Mg	Al	Ca	Cr	Mn	Fe	Ni	Cu
1	1.1 x 10 <sup>-1</sup>	<10 <sup>-2</sup>	<10 <sup>-2</sup>	<10 <sup>-2</sup>	<10 <sup>-3</sup>	1.1 x 10 <sup>-2</sup>	3.7 x 10 <sup>-2</sup>	<10 <sup>-2</sup>	<10 <sup>-2</sup>
2	1.0 x 10 <sup>-1</sup>	<10 <sup>-2</sup>	<10 <sup>-2</sup>	<10 <sup>-2</sup>	<10 <sup>-3</sup>	1.2 x 10 <sup>-2</sup>	4.2 x 10 <sup>-2</sup>	<10 <sup>-2</sup>	<10 <sup>-2</sup>
3	NA	<10 <sup>-2</sup>	<10 <sup>-2</sup>	<10 <sup>-2</sup>	<10 <sup>-3</sup>	1.2 x 10 <sup>-2</sup>	4.4 x 10 <sup>-2</sup>	<10 <sup>-2</sup>	<10 <sup>-2</sup>
4	NA	<10 <sup>-2</sup>	<10 <sup>-2</sup>	<10 <sup>-2</sup>	<10 <sup>-3</sup>	1.2 x 10 <sup>-2</sup>	4.3 x 10 <sup>-2</sup>	<10 <sup>-2</sup>	<10 <sup>-2</sup>
5	1.1 x 10 <sup>-1</sup>	<10 <sup>-2</sup>	<10 <sup>-2</sup>	<10 <sup>-2</sup>	<10 <sup>-3</sup>	1.3 x 10 <sup>-2</sup>	4.4 x 10 <sup>-2</sup>	<10 <sup>-2</sup>	<10 <sup>-2</sup>
6	1.0 x 10 <sup>-1</sup>	<10 <sup>-2</sup>	<10 <sup>-2</sup>	<10 <sup>-2</sup>	<10 <sup>-3</sup>	1.2 x 10 <sup>-2</sup>	4.2 x 10 <sup>-2</sup>	<10 <sup>-2</sup>	<10 <sup>-2</sup>
7	9.0 x 10 <sup>-2</sup>	<10 <sup>-2</sup>	1.6 x 10 <sup>-2</sup>	<10 <sup>-2</sup>	<10 <sup>-3</sup>	8.9 x 10 <sup>-3</sup>	3.8 x 10 <sup>-2</sup>	<10 <sup>-2</sup>	<10 <sup>-2</sup>
8	2.1 x 10 <sup>-1</sup>	NM	NM	NM	NM	NM	4.7 x 10 <sup>-2</sup>	NM	NM
9	2.2 x 10 <sup>-1</sup>	NM	NM	NM	NM	NM	5.3 x 10 <sup>-2</sup>	NM	NM
10	2.4 x 10 <sup>-1</sup>	NM	NM	NM	NM	NM	4.2 x 10 <sup>-2</sup>	NM	NM
11	1.7 x 10 <sup>-1</sup>	NM	NM	NM	NM	NM	4.8 x 10 <sup>-2</sup>	NM	NM

<sup>a</sup>A value with "<" means that the concentration of that species in the organic phase was below its detection limit. The value given is the detection limit divided by its aqueous-phase concentration.

<sup>b</sup>NA means not analyzed; NM means that the concentration of a species was below the detection limit in both phases.

<sup>c</sup>Stage 7 is the feed stage; stages 1-7 are extraction stages; stages 8 and 9 are scrub 1 stages; and stages 10 and 11 are scrub 2 stages.

<sup>d</sup>H<sub>2</sub>O<sub>x</sub> = oxalic acid. The distribution ratio was measured by adding <sup>14</sup>C-labeled oxalic acid to the near steady-state solutions of the cold countercurrent run and equilibrating them at 40°C.

TABLE X

## DISTRIBUTION RATIOS OF FISSION PRODUCTS IN EACH STAGE OF THE COUNTERCURRENT EXPERIMENT

Stage No.	Distribution Ratio <sup>a,b</sup>								
	Sr	Y	Zr	Mo	Tc <sup>c</sup>	Ru	Rh	Pd	Ag
1	<10 <sup>-2</sup>	1.4	3.3 x 10 <sup>-3</sup>	<10 <sup>-1</sup>	2.7	3.4 x 10 <sup>-2</sup>	<10 <sup>-1</sup>	<10 <sup>-1</sup>	<10 <sup>-1</sup>
2	<10 <sup>-2</sup>	1.4	7.1 x 10 <sup>-3</sup>	<10 <sup>-1</sup>	2.2	3.4 x 10 <sup>-2</sup>	<10 <sup>-1</sup>	<10 <sup>-1</sup>	<10 <sup>-1</sup>
3	<10 <sup>-2</sup>	1.4	1.2 x 10 <sup>-2</sup>	<10 <sup>-1</sup>	NA	3.4 x 10 <sup>-2</sup>	<10 <sup>-1</sup>	<10 <sup>-1</sup>	<10 <sup>-1</sup>
4	<10 <sup>-2</sup>	1.4	1.2 x 10 <sup>-2</sup>	<10 <sup>-1</sup>	NA	3.3 x 10 <sup>-2</sup>	<10 <sup>-1</sup>	<10 <sup>-1</sup>	<10 <sup>-1</sup>
5	<10 <sup>-2</sup>	1.4	1.7 x 10 <sup>-2</sup>	<10 <sup>-1</sup>	2.6	6.8 x 10 <sup>-2</sup>	<10 <sup>-1</sup>	<10 <sup>-1</sup>	<10 <sup>-1</sup>
6	<10 <sup>-2</sup>	1.3	1.6 x 10 <sup>-2</sup>	1.0 x 10 <sup>-1</sup>	2.9	1.1 x 10 <sup>-1</sup>	<10 <sup>-1</sup>	1.7 x 10 <sup>-1</sup>	<10 <sup>-1</sup>
7	<10 <sup>-2</sup>	1.1	1.1 x 10 <sup>-2</sup>	1.1 x 10 <sup>-1</sup>	3.6	3.5 x 10 <sup>-1</sup>	1.1 x 10 <sup>-1</sup>	2.6 x 10 <sup>-1</sup>	<10 <sup>-1</sup>
8	NM	1.2	1.6 x 10 <sup>-1</sup>	NM	2.3	1.2	NM	5.4 x 10 <sup>-1</sup>	NM
9	NM	1.3	NM	NM	2.0	2.3	NM	1.0	NM
10	NM	1.2	NM	NM	7.0 <sup>d</sup>	3.0	NM	1.0	NM
11	NM	1.0	NM	NM	NA	3.0	NM	1.0	NM

(Cont'd)

**TABLE X (Cont'd)**

Stage No.	Distribution Ratio <sup>a,b</sup>								
	Cd	Te	Ba	La	Ce	Pr	Nd	Sm	Eu
1	<10 <sup>-2</sup>	<10 <sup>-2</sup>	<10 <sup>-2</sup>	NM	NM	NM	NM	NM	NM
2	<10 <sup>-2</sup>	<10 <sup>-2</sup>	<10 <sup>-2</sup>	NM	NM	NM	NM	NM	NM
3	<10 <sup>-2</sup>	<10 <sup>-2</sup>	<10 <sup>-2</sup>	3.2	NM	NM	NM	NM	NM
4	<10 <sup>-2</sup>	<10 <sup>-2</sup>	<10 <sup>-2</sup>	3.4	NM	NM	NM	NM	NM
5	<10 <sup>-2</sup>	<10 <sup>-2</sup>	<10 <sup>-2</sup>	3.7	4.6	NM	NM	5.3	4.0
6	<10 <sup>-2</sup>	<10 <sup>-2</sup>	<10 <sup>-2</sup>	3.5	5.1	6.4 <sup>e</sup>	4.4 <sup>e</sup>	5.8	4.2
7	<10 <sup>-2</sup>	<10 <sup>-2</sup>	<10 <sup>-2</sup>	2.9	4.5	5.2 <sup>e</sup>	4.7 <sup>e</sup>	5.1	4.2
8	NM	NM	NM	3.7	6.3	7.0	7.0	7.0	5.6
9	NM	NM	NM	4.2	7.3	8.1	8.3	8.2	7.0
10	NM	NM	NM	4.2	8.7	9.6	9.5	9.5	7.7
11	NM	NM	NM	4.8	7.7	8.1	7.8	7.8	6.2

<sup>a</sup>A value with "<" means that the concentration of that species in the organic phase was below its detection limit. The value given is the detection limit divided by its aqueous-phase concentration.

<sup>b</sup>NA means not analyzed; NM means that the concentration of a species was below the detection limit in both phases.

<sup>c</sup>The technetium distribution ratio analysis was performed by taking the near-steady-state solutions from the cold countercurrent run, spiking them with <sup>99</sup>Tc, and equilibrating them at 40°C.

<sup>d</sup>A second contact of the organic phase with unspiked, fresh aqueous phase gave a technetium distribution ratio of 11.7.

<sup>e</sup>Interference in the atomic emission lines for these elements puts these values in doubt.

were close to those predicted from batch distribution ratio measurements.<sup>2,3]</sup> Data for ruthenium and palladium indicate the presence of at least two species with different distribution ratios. In summary, the distribution ratios were such that all metal ions but the rare earth elements and technetium were discharged with the raffinate.

Although technetium was found predominantly in the loaded organic phase, the agreement between the measured concentration of technetium and that calculated based on  $D_{Tc}$  in the raffinate samples is not good, as shown in Figure 8. The reasons for the disparity is not certain. A more detailed analysis of the technetium data can be found.<sup>2]</sup> The calculated steady-state concentration of technetium in the raffinate predicts that 89% of the technetium reports to the organic phase. The removal of technetium from the raffinate is considered advantageous because its presence in nonTRU waste can complicate disposal.

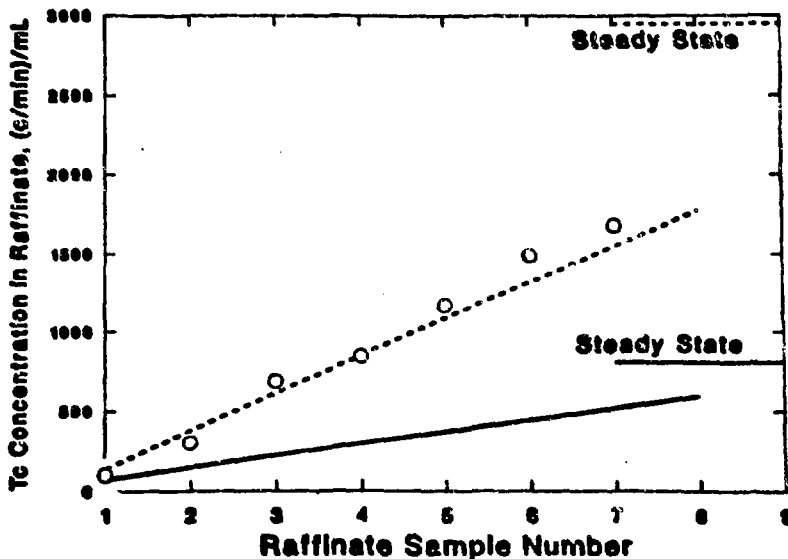


Figure 8. Raffinate concentration of  $^{99}Tc$  vs. the raffinate sample number. (The data are measured raffinate concentrations, the solid line is calculated from measured distribution ratios, and the dashed line is an empirical fit of the data.)

### 3.3 Stripping Properties of TRUEX Solvent

The results of stripping experiments, which are presented in detail elsewhere,<sup>2,3</sup> indicate that a double strip is necessary and, perhaps, even an advantage of the process. A dilute acid strip is sufficient to strip americium and the rare earths from the TRUEX solvent. For example, the americium concentration in the loaded solvent was reduced by  $5 \times 10^3$  in six successive batch contacts using strip solution 1. The rare earths were undetectable (as oxalate precipitate) in the aqueous phase after the fifth strip. Ten successive strips reduced the americium concentration by  $\sim 10^6$ .

An efficient separation of americium from plutonium and neptunium can be achieved by eliminating HAN from the dilute nitric acid strip. The value of the separation factor, Pu(IV)/Am(III), is  $\sim 10^3$ . After stripping Am(III), Pu(IV) and Np(IV) can be removed with HNO<sub>3</sub>-HF. Any uranium present in the organic phase can be removed during the solvent cleanup step.

### 3.4 Phase-Disengagement Behavior

The phase-separation times for all extraction, scrub, and strip stages were within one minute. No interfacial crud was observed in any of the stages and all solutions were generally very clear, indicating little entrainment. Thus, the TRUEX process seems well suited to a continuous countercurrent operation.

## 4. SUMMARY AND CONCLUSIONS

The data in Tables IV, V, and VI show quite clearly that the TRUEX process is not only capable of efficiently reducing the TRU content of a simulated HLW solution to less than 100 nCi/g of solid raffinate, but also that it is capable of reducing the



quantity of TRU waste by more than two orders of magnitude. In addition, the separation of americium from plutonium and neptunium is feasible by a two-step stripping operation. Removal of all TRU elements from the solvent phase by solvent recycle is sufficiently complete that treatment of spent TRUOX solvent with Amberlyst A-26 resin in the hydroxide cycle will likely restore the solvent to prime condition.<sup>9]</sup>

Figure 9 shows a modified TRUOX flowsheet for DSX that incorporates improvements developed as a result of the cold and hot countercurrent experiments.

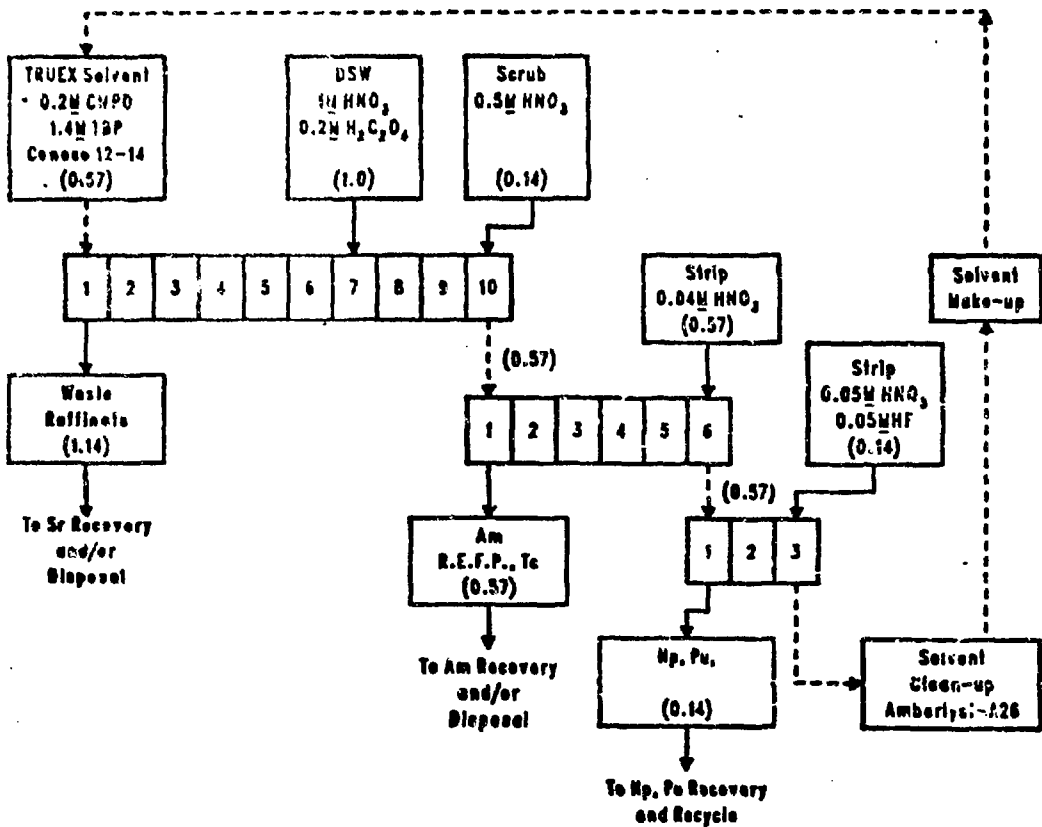


Figure 9. An improved CMPO-TRUOX flowsheet for DSX feed. (Numbers in parentheses indicate relative flow rates.)

## 5. ACKNOWLEDGMENTS

The authors would like to acknowledge the help of P. R. Danesi, Chemistry Division, ANL, and R. Chiarizia, Chemistry Division, ENEA-Casaccia, Rome, Italy, in performing the laboratory batch countercurrent experiments and the efforts of E. L. Callis, A. M. Essling, and E. A. Huff, Analytical Chemistry Laboratory, ANL, in providing analytical data.

Funding for this effort was shared jointly by the DOE Division of Basic Energy Sciences and Rockwell Hanford Operations.

## 6. LITERATURE CITED

1. 10 CFR 61, "Licensing Requirements for Land Disposal of Radioactive Waste," U.S. Nuclear Regulatory Commission, Final Rule (October 1982).
2. Vandegrift, G. F.; Leonard, R. A.; Steindler, M. J.; Horwitz, E. P.; Basile, L. J.; Diamond, H.; Kalina, D. G.; Kaplan, L., "Transuranic Decontamination of Nitric Acid Solutions by the TRUOX Solvent Extraction Process - Preliminary Development Studies," ANL-84-45 (July 1984).
3. Horwitz, E. P.; Kalina, D. G.; Diamond, H.; Vandegrift, G. F.; Shultz, W. W., "The TRUOX Process - A Process for the Extraction of the Transuranic Elements from Nitric Acid Wastes Utilizing Modified PUREX Solvent," accepted for publication *Solv. Extr. Ion Exchange*.
4. Peppard, D. F., "Liquid-Liquid Extraction of Metal Ions," in Advances in Inorganic and Radiochemistry, Vol. 9, Academic Press, Inc., New York (1966).
5. Huff, E. A.; Horwitz, E. P., "ICP-AES in Support of Nuclear Waste Management," *Spectrochem. Acta*, 40B, 279 (1985).

6. Leonard, R. A., "Use of Electronic Worksheets for Calculation of Stagewise Solvent Extraction Processes," submitted for presentation at the Symposium on Separation Science and Technology for Energy Application, Knoxville, TN (October 20-24, 1985).
7. Alders, L. L., Liquid-Liquid Extraction, 2nd ed., Elsevier Science Publishers, New York, 1959.
8. Treybal, R. E., Liquid Extraction, 2nd ed., McGraw-Hill Book Co., New York (1963).
9. Schulz, W. W., "Macroreticular Ion-Exchange Resin Cleanup of PUREX Process TBP Solvent," Proc. Int. Solv. Extr. Conf., Vol. I, Society of Chemical Industry, London, 174 (1971.)